Progress In Electromagnetics Research, Vol. 132, 603–619, 2012

TUBULAR LINEAR INDUCTION MACHINE AS A FAST ACTUATOR: ANALYSIS AND DESIGN CRITERIA

A. Musolino, R. Rizzo*, and E. Tripodi

Department of Energy and System Engineering, University of Pisa, Via Diotisalvi 2, Pisa 56126, Italy

Abstract—In this paper, some design criteria for a Tubular Linear Induction Motor (TLIM) as a fast actuator are considered. The influence of geometrical and physical parameters on the operating conditions of a TLIM are investigated by means a quasi-analytic model. The model is based on the application of the Fourier Transform both in space and in time. The Fourier transform in space is introduced to take into account the finite length of the stator windings in the axial direction. The transient electrical response of the motor at standstill following the insertion of a three-phase system of voltage generators is performed by the Fourier transform in the time.

1. INTRODUCTION

Linear movements are very usual in mechanical engineering, especially in industrial robots, where linear speeds up to several meters per second are often required. These movements are usually obtained by using rotating motors in combination with rotation to translation mechanism. The resulting systems may have poor performance; in particular, an excessive time delay may prevent their use as fast actuators [1]. The complexity of these systems can be overcome by using linear actuators. It is well known that tubular linear induction machines have the highest force to moving mass ratio when compared with other linear motors; this property makes these devices very attractive to be used as servo motors since they may have better performance in terms of reduction of delay times with respect to those of traditional systems.

The simplest approach to model these linear motors is based on the use of lumped equivalent circuits as described in [1–7] for similar

Received 15 September 2012, Accepted 15 October 2012, Scheduled 19 October 2012

* Corresponding author: Rocco Rizzo (rocco.rizzo@dsea.unipi.it).

devices. However, while this technique allows to establish analytical relationships between the design parameters and the performance of the machine, it suffers from inherent inaccuracy especially in presence of complex flux paths.

A step forward can be performed by means of analytical methods which provide simple closed formulas for a quick evaluation of the distribution of magnetic flux density and induced currents as a function of the machine's dimensions and of the slip [8, 9].

More accurate design requires the development of 3D models of the motors that allow to determine the distribution of electrical and mechanical quantities taking into account the finite length of the machine, the presence of slots and teeth, the presence of nonlinear materials and the transient nature of the phenomena that take place in these devices [10–19]. Numerical method based on integral formulation may be convenient in the analysis of such devices because of the presence of conductors in motion. Integral formulation do not suffer of some of the drawbacks of Finite Elements Methods (FEM) related to the sliding meshes [20–26], but may require long computation times. Many integral formulations reduce the analysis of the device to the one of an equivalent network. It is worthwhile to note that these formulations allow for a quick and accurate evaluation of the sensitivity with respect to the design parameters [27, 28].

Numerical approaches are time consuming (especially when used in conjunction with automatic optimizers) and they are not effective to insight the dependence of the performance on the design parameters.

The use of more sophisticated analytical models characterized by series expansions of the solution in terms of special functions may represent a good compromise between accuracy and requested computation time.

The design of a TLIM as a fast actuator cannot leave its time response out of consideration. This time depends on the weight of the mover and on the waveform of the thrust force acting on it at standstill.

In this paper a quasi analytical model of a TLIM based on the use of a double Fourier Transform, is used to obtain the transient behavior of the main electromechanical quantities following the insertion of a three phase voltage generator. The solution of the governing equations in the transformed domain is expressed in terms of Bessel functions. The numerical inverse transform allows to determine the distribution of all the electrical and mechanical quantities and to specify some design criteria for a TLIM as fast actuator.

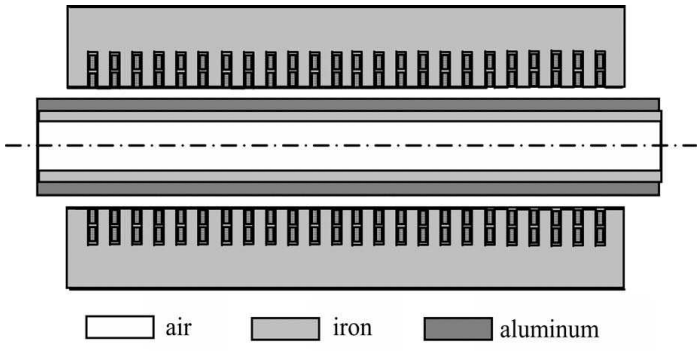

Figure 1. Schematization of the TLIM with hollowed mover.

2. THE MODEL

A schematization of a TLIM is shown in Fig. 1. The armature consists of a conductive nonferromagnetic sheet (aluminum) surrounding an iron tube. The whole armature is free to move in the axial direction on linear bearings [29] (not shown in the figure).

2.1. Governing Equation

Because of the presence of slots and teeth, the device shown in Fig. 1 can only be analyzed by numerical methods. Analytical models can be obtained by using a simplified structure with a smooth stator and with the primary windings substituted by an equivalent current sheet. The use of the Carter coefficient allows to evaluate the equivalent air gap and a proper positioning of the current sheet [30–32]. Defining g_0 as the distance between the iron-massive part of the mover and the inner part of the stator, the Carter airgap is given by:

$$g_C = \frac{\tau_{cv}}{\tau_{cv} - \gamma\tau_0} g_0; \quad \text{with} \quad \gamma = \frac{(b_{cv}/g_0)^2}{(5 + (b_{cv}/g_0))}; \tag{1}$$

where τ_{cv} and b_{cv} are respectively the distance between two adjacent slots and the axial width of the slots as shown in Fig. 2.

The model so obtained does correctly work as far as the motor is fed by imposed currents. When the motor is fed by a three phase voltage generator, a set of inductors and resistors has to be series connected to the equivalent impedance of the motor in order to take into account the voltage drops due the resistance of the conductors and to the leakage fluxes in the slots.

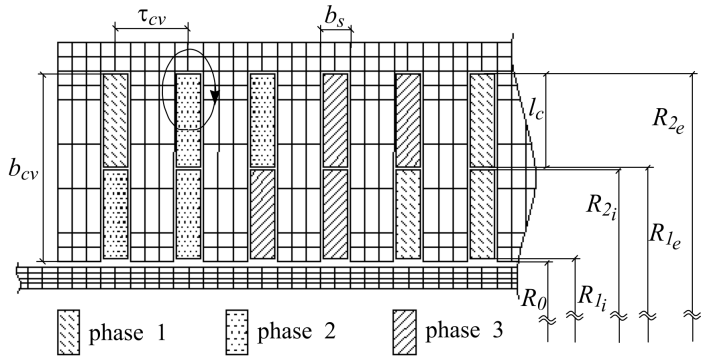

Figure 2. Double layer winding of a TLIM.

The resistors are evaluated by using the d.c. values, while the evaluation of the inductors has been performed by using a classical approach taken from electrical machines textbooks [30, 31].

For the sake of simplicity we consider a double layered primary winding as shown in Fig. 2. In this case we consider only the coupling between coils in the same slot, and assume that coils in different slots are not magnetically coupled. Let L_i the inductance of the coil in the inner position in a slot and L_e the inductance of the one in the external position; $M_{i,e}$ is the mutual inductance between the two coils. We can write:

$$L_{i/e} = \frac{2 \cdot W_{i/e}}{i_{i/e}^2}; \quad \text{and} \quad M_{i,e} = \frac{W_{i,e}}{i_i \cdot i_e}; \tag{2}$$

where:

$$W_{i/e} = \frac{\mu_0 \pi N^2 i_{i,e}^2}{b_s} \left\{ \frac{1}{l_c^2} \left[\frac{1\left(R_{2_{i/e}}^4 - R_{1_{i/e}}^4\right)}{4} - \frac{2R_{2_{i/e}}\left(R_{2_{i/e}}^3 - R_{1_{i/e}}^3\right)}{3} + \frac{R_{2_{i/e}}^2\left(R_{2_{i/e}}^2 - R_{1_{i/e}}^2\right)}{2} \right] + \frac{R_{1_{i/e}}^2 - R_0^2}{2} \right\};$$

$$W_{i,e} = \frac{2\mu_0 \pi N^2 i_i i_e}{b_s} \left\{ -\frac{1}{l_c^2} \left[\frac{\left(R_{2_i}^3 - R_{1_i}^3\right)}{3} - \frac{R_{2_i}\left(R_{2_i}^2 - R_{1_i}^2\right)}{2} \right] + \frac{R_{1_i}^2 - R_0^2}{2} \right\};$$

The notation i/e means that the subscript may assume the value i or e. The above equations are obtained by considering the flux density distribution evaluated under the hypothesis $\mu_{fe} = \infty$ and by using

closed paths as the one shown in Fig. 2 [30, 31]. Subscript 2 and 1 respectively refer to the outer and inner radius of each coil. N is the number of turns, R_0 is the inner radius of the slot and b_s and l_c are the linear dimensions of the slot and coil as shown in Fig. 2.

Considering the winding scheme in Fig. 2, the inductance of the section of a winding located in three adjacent slots is:

$$L_{sect} = 2 \cdot (L_i + L_e + M_{i,e}); \tag{3}$$

The total voltage drop on the leakage inductance of each phase is written as the sum of one term due to the current in that phase, and of two terms due to the coupling with the currents in the other phases. If the motor is fed by a three phase balanced system of currents, we can write: $I_2 = I_1 e^{j2\frac{\pi}{3}}$ and $I_3 = I_1 e^{j4\frac{\pi}{3}}$ and as a consequence:

$$\begin{aligned} V_1 &= j\omega N_{sect} \cdot (L_{sect} I_1 \pm M_{i,e} I_2 \pm M_{i,e} I_3) \\ &= j\omega N_{sect} \cdot \left(L_{sect} I_1 \pm M_{i,e} I_1 e^{j2\frac{\pi}{3}} \pm M_{i,e} I_1 e^{j4\frac{\pi}{3}} M_{i,e} \right) \\ &= j\omega N_{sect} \cdot \left(L_{sect} \pm M_{i,e} e^{j2\frac{\pi}{3}} + \pm M_{i,e} e^{j4\frac{\pi}{3}} M_{i,e} \right) I_1 = j\omega L_{tot} I_1; \end{aligned} \tag{4}$$

where N_{sect} represents the number of series connected sections of a given phase that constitute the entire winding; throughout the paper we assume $N_{sect} = 4$. The choice of the sign in (5) depends on the relative direction of the turns of the coils in the same slot.

The same inductors have also been evaluated by using the computer codes in [10, 15], and the difference between the two numerical values and those by the above formulas is within $\pm 5\%$.

A number of analytical models of TLIM when fed by a current sheet are derived under the hypothesis of indefinite axial length of the machine and in steady operating conditions [3, 8, 9]. A quasi-analytical model is used here to approximate the finite length of the stator by considering a finite axial extension of the primary currents windings and an indefinite length of the primary core [33–35]. End effects are therefore caused only by the finite length of the primary windings but not by the iron core. Let the primary current sheet extend between $z = 0$ and $z = L$.

Figure 3 shows a schematic representation of the motor used for the deduction of the quasi-analytical model.

Introducing in the Maxwell equations the vector potential with the Coulomb gauge, for field equation of an isotropic medium moving with velocity [8] we can write:

$$\nabla^2 \bar{A} = \mu\sigma \left(\frac{\partial}{\partial t} \bar{A} - v \times \left(\nabla \times \bar{A} \right) \right) \tag{5}$$

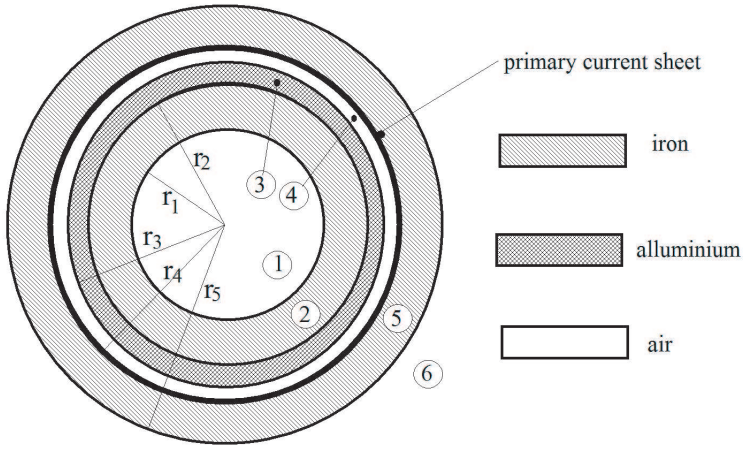

Figure 3. Linear tubular machine scheme.

where μ and σ respectively indicate the permeability and the conductivity of the medium. In the following analysis we assume that the permeability of the iron is constant. This hypothesis is based on the greater length of the air gap of linear motors in comparison with that of rotating induction motors.

In a cylindrical coordinates system we can express the primary current sheet as follows:

$$\bar{J}_1(r,\varphi,z,t) = J_1 \sin(\omega t - kz)u(z)u(L-z)\delta(r-r_4)\cdot\bar{a}_\varphi \qquad (6)$$

where $\bar{a}_\varphi$ indicates the azimuth direction, $u(z)$ is the unit step function and $\delta(r-r_4)$ is the Dirac function located on the inner face of the stator. Let p the number of the poles of the motor, then $k = 2p\pi/L$.

Vector potential has only azimuth components in cylindrical coordinates and is a function of r, z and t: $\bar{A} = A_\varphi(r,z,t)\cdot\bar{a}_\varphi$.

Substituting in (1), after some manipulations we obtain:

$$\frac{\partial^2 A_\varphi}{\partial r^2} + \frac{1}{r}\frac{\partial A_\varphi}{\partial r} + \frac{\partial^2 A_\varphi}{\partial z^2} - \frac{A_\varphi}{r^2} = \mu\sigma\left(\frac{\partial A_\varphi}{\partial t} + v_z\frac{\partial A_\varphi}{\partial z}\right) \qquad (7)$$

On sinusoidal steady state condition the vector potential is expressed as: $A_\varphi(r,z,t) = A_\varphi(r,z)\cdot e^{j\omega t}$. Substituting in (7) we obtain:

$$\frac{\partial^2 A_\varphi}{\partial r^2} + \frac{1}{r}\frac{\partial A_\varphi}{\partial r} + \frac{\partial^2 A_\varphi}{\partial z^2} - \frac{A_\varphi}{r^2} = \mu\sigma\left(j\omega A_\varphi + v_z\frac{\partial A_\varphi}{\partial z}\right) \qquad (8)$$

Let the Fourier transform of $A_\varphi\,(r,\ z)$ with respect to z be denoted

by $\tilde{A}_\varphi(r,\zeta)$:

$$A_\varphi(r,z) = \frac{1}{2\pi}\int_{-\infty}^{+\infty} \tilde{A}_\varphi(r,\zeta)e^{j\zeta z}d\zeta \tag{9}$$

Then in terms of Fourier transform, (8) becomes:

$$\frac{\partial^2 \tilde{A}_{i,\varphi}}{\partial r^2} + \frac{1}{r}\frac{\partial \tilde{A}_{i,\varphi}}{\partial r} - \left(\zeta^2 + \frac{1}{r^2}\right)\tilde{A}_{i,\varphi} = j\mu\sigma\left(\omega - \zeta v_z\right)\tilde{A}_{i,\varphi} \tag{10}$$

Subscript i is introduced according to Fig. 3 to indicate the regions where (10) is written. Writing (10) in the regions labeled with 1, 2, 4, 5, 6 where $\sigma = 0$ or $v_z = 0$ (iron cores and air) we obtain:

$$\frac{\partial^2 \tilde{A}_{i,\varphi}}{\partial r^2} + \frac{1}{r}\frac{\partial \tilde{A}_{i,\varphi}}{\partial r} - \left(\zeta^2 + \frac{1}{r^2}\right)\tilde{A}_{i,\varphi} = 0; \quad \text{for} \quad i \neq 3; \tag{11}$$

In the conductive region of the mover we have:

$$\frac{\partial^2 \tilde{A}_{i,\varphi}}{\partial r^2} + \frac{1}{r}\frac{\partial \tilde{A}_{i,\varphi}}{\partial r} - \left(j\alpha^2 + \frac{1}{r^2}\right)\tilde{A}_{i,\varphi} = 0; \quad \text{for} \quad i = 3; \tag{12}$$

where: $\alpha^2 = \zeta^2(s\frac{\mu\sigma v_s}{\zeta} - j)$, and s is the slip of the mover with respect to the current wave of wavelength $2\pi/\zeta$, whose synchronous speed is $v_s(\zeta) = \omega/\zeta$.

2.2. Solution of the Governing Equation

Solutions of Equations (11) and (12) are expressed in terms of modified Bessel functions of the first and second kind [36]:

$$\tilde{A}_{i,\varphi} = c_i I_1(\zeta r) + c_i' K_1(\zeta r); \quad \text{for} \quad i \neq 3 \tag{13}$$

$$\tilde{A}_{3,\varphi} = c_3 I_1(\sqrt{j}\alpha r) + c_3' K_1(\sqrt{j}\alpha r); \quad \text{for} \quad i = 3 \tag{14}$$

The determination of the unknown coefficients in the previous relations is obtained by imposing the following boundary conditions:

$$\begin{aligned}
&\tilde{B}_{i,r}(r,z) = \tilde{B}_{i+1,r}(r,z); \quad \text{for} \quad i = 1,\ldots,6; \quad \text{and} \quad r = r_1,\ldots,r_5;\\
&\tilde{H}_{i,r}(r,z) = \tilde{H}_{i+1,r}(r,z); \quad \text{for} \quad i \neq 4; \quad \text{and} \quad r \neq r_4;\\
&\tilde{H}_{4,r}(r,z) - \tilde{H}_{5,r}(r,z) = \tilde{J}_1; \quad \text{for} \quad r = r_4;
\end{aligned} \tag{15}$$

where $\tilde{J}_1(\zeta)$ is the Fourier transform of the excitation current.

In order to obtain the integration coefficients c_i and c_i', the fields $\tilde{B}$ and $\tilde{H}$ are expressed in terms of vector potential $\tilde{A}$. Before solving the resultant linear system for the determination of the integration constants let us observe that $c_1' = c_6 = 0$ because of the form of the

modified Bessels functions. Then the other coefficients can be written in the form:

$$c_i = \tilde{J}_1(\zeta)\frac{N_i(\zeta)}{D_i(\zeta)}; \qquad c'_i = \tilde{J}_1(\zeta)\frac{N'_i(\zeta)}{D'_i(\zeta)}; \tag{16}$$

where $N_i(\zeta)$, $D_i(\zeta)$, $N'_i(\zeta)$ and $D'_i(\zeta)$ are involved expressions containing Bessel functions. Finally a numerical Fourier inverse transform allows obtaining the vector potential and all the others electromagnetic quantities in the whole space. In particular, the induced eddy currents in the aluminum are found as:

$$\bar{J} = \sigma\bar{E} = -j\sigma\,(\omega - \alpha v_z)\cdot\bar{A};$$

and the total thrust force is expressed by:

$$\bar{F} = \frac{1}{2}\int_V \Re\big(\bar{J}\times\bar{B}^*\big)dv;$$

where V is the conductive cylinder.

It is now possible to evaluate the voltages at the terminals of the stator windings at the arbitrary angular frequency ω. The calculation is carried out by firstly performing a line integration of the vector potential on circular lines located on the current sheet and corresponding to the turns of the windings.

These lines and their orientations are determined by considering the position of the stator conductors inside the slots and the direction in which they are wound. The axial position of a turn of a coil ranges within the z coordinates corresponding to the middle points of the teeth that delimit the slot where the coil is located.

In order to evaluate the resultant e.m.f. at the terminal of each winding the contributions of the turns are summed considering the coils interconnection in the winding scheme.

We can write:

$$\begin{aligned} E_i(\omega) &= j\omega\sum_{k=1}^{N^i_{coil}}\frac{\alpha^i_k N^i_{cond,k}}{z_{zk}-z_{1k}}\int_0^{2\pi}\int_{z_{1k}}^{z_{2k}} A_\varphi(r_4,z)r_4 d\theta dz \\ &= j\omega 2\pi r_4\sum_{k=1}^{N^i_{coil}}\frac{\alpha^i_k N^i_{cond,k}}{z_{zk}-z_{1k}}\int_{z_{1k}}^{z_{2k}} A_\varphi(r_4,z)dz; \quad \text{for} \quad i=1,\ldots,3; \end{aligned} \tag{17}$$

In the above expression N^i_{coil} and $N^i_{cond,k}$ are respectively the number of coil in the ith winding and the number of the conductors of the kth coil of the ith winding. The coefficient α^i_k assumes the values ± 1 depending on the direction of the turns in the kth coil of the ith winding.

To obtain the voltages at the terminal of the real windings we have to add to the electromotive force the contributes due to the voltage drops on the resistors and on the inductors produced by the currents in the windings. These currents can be evaluated as:

$$I = \frac{2J_1}{N_{tot\ cond}} \frac{\sin\left(\frac{2p\pi}{2N_{tot\ slot}}\right)}{\frac{2p\pi}{L}}; \tag{18}$$

where $N_{tot\ slot}$ is the total number of slots in the motor and $N_{tot\ cond}$ the total number of conductor in a slot. The slots have the same dimensions and are equally spaced along the axial direction and with the same total number of conductors inside them.

It is now possible to write for the voltages at the terminals of the windings the following expressions:

$$\dot{V}_i(\omega) = \dot{E}_i(\omega) + R_i\dot{I}_i(\omega) + j\omega L_i\dot{I}_i(\omega) = \bar{Z}_i(\omega)\dot{I}_i(\omega); \tag{19}$$

Once the impedance of each phase of the motor is known it is possible to determine the absorbed currents when the motor is fed by a three phase voltage generator at arbitrary frequency.

Because of the finite length of the motor the impedances $\bar{Z}_i$ are slightly different, so that the currents in the windings are not able to produce the same magneto-motive force as that produces by (6). At a first approximation we can neglect this error which decreases with the length of the motor and its number of pole pairs.

Lets now consider the insertion of a three phase symmetric voltage generator of the form:

$$\begin{aligned} v_1(t) &= V_M \sin(\omega_0 t + \varphi) \cdot u(t) \\ v_2(t) &= V_M \sin\left(\omega_0 t + \varphi - \frac{2\pi}{3}\right) \cdot u(t) \\ v_3(t) &= V_M \sin\left(\omega_0 t + \varphi - \frac{4\pi}{3}\right) \cdot u(t) \end{aligned} \tag{20}$$

Let $\tilde{V}_1(\omega)$, $\tilde{V}_2(\omega)$ and $\tilde{V}_3(\omega)$ respectively be the Fourier transforms of the applied voltages. The feeding voltages can be expressed as:

$$\begin{aligned} v_1(t) &= \sum_n \left\|\tilde{V}_1(\omega_n)\right\| \cdot \Delta\omega_n \cdot \sin\left(\omega_n t + \angle\tilde{V}_1(\omega_n)\right) \\ v_2(t) &= \sum_n \left\|\tilde{V}_2(\omega_n)\right\| \cdot \Delta\omega_n \cdot \sin\left(\omega_n t + \angle\tilde{V}_2(\omega_n)\right) \\ v_3(t) &= \sum_n \left\|\tilde{V}_3(\omega_n)\right\| \cdot \Delta\omega_n \cdot \sin\left(\omega_n t + \angle\tilde{V}_3(\omega_n)\right) \end{aligned} \tag{21}$$

Once the phasors $\dot{V}_i = \|\tilde{V}_i(\omega_n)\| \cdot \Delta\omega_n e^{j\angle V_i(\omega_n)}$, corresponding to the nth harmonic component, are known, Equation (19) can be used to obtain the absorbed currents and correspondingly all the electromechanical quantities in the motor at ω_n. We are so able to study of the transient phenomena in the TLIM at standstill following the insertion of a three phase voltage generator. The extension to feeding generators of arbitrary waveform is straightforward. If the feeding voltages in (20) are periodic waveforms with the same period, using the Fourier transform expressions as in (21) are obtained. In the most general case, the three phasors at the angular frequency ω_n do not constitute a set of symmetrical voltages. However, if we use the Fortescue theorem these three phasors can be resolved into three balanced system of phasors: positive, negative and zero sequence components so that we can use the previously described method.

3. RESULTS

The proposed model has been used to characterize the operating condition of a TLIM in order to obtain design criteria. The linear dependence of the thrust force on the length of the motor can be assumed for realistic length-to-radius ratio of the motor. This linear dependence is obtained when the feeding voltages are proportional to the length of the motor.

3.1. Transient Response

Results here presented refer to a motor with a stator of length 32.4 cm and with two pole pairs obtained by a double layered winding as shown in Fig. 2. Because of the presence in the mover of a conductive non ferromagnetic cylinder the reluctance of the magnetic circuits of the motor can assume high values. As a consequence the leakage fluxes in the slots can assume comparable values with those of the flux in the mover. A careful design of the stator is important in order to keep as small as possible the leakage fluxes. Wide and superficial slots should be used, and this is helpful in reducing the radial dimension of the motor. Moreover slots so shaped may cause high values of the Carter coefficient and produce reduced thrust force at a given absorbed current. On the other hand we have to consider that reducing the leakage impedance, the absorbed current at a given feeding voltage is increased. Figs. 4(a)–4(c) show the waveforms of the thrust force on the mover for different shapes of the slots and for different external radii of the mover. The conductor on the mover is supposed to be aluminum ($\sigma = 3.57 \times 10^7$ S/m) and is 2 mm thick; the same thickness

is assumed for the iron on the mover. We consider the standstill condition and evaluate the transient response to the insertion of a 220 V balanced three-phase feeding voltage generator at 50 Hz. The generators have the waveforms as in (20); the response cannot by obtained by considering the steady behaviour at 50 Hz but we have to sum the contributes of the terms in (21) that represents the non sinusoidal feeding voltage as the sum of sinusoidal components at different frequencies.

As expected the figures show an increased force with the length of the slots (in the Figs. 4(a) to 4(a) the area of the cross section of the slot is approximately the same). These results show an increasing thrust force with a decreasing radius of the motor. This can be explained remembering that the feeding voltage is the same in the three cases.

Reducing its radius, the motor produces a reduction of its total impedance and a corresponding increment of the current. At a first

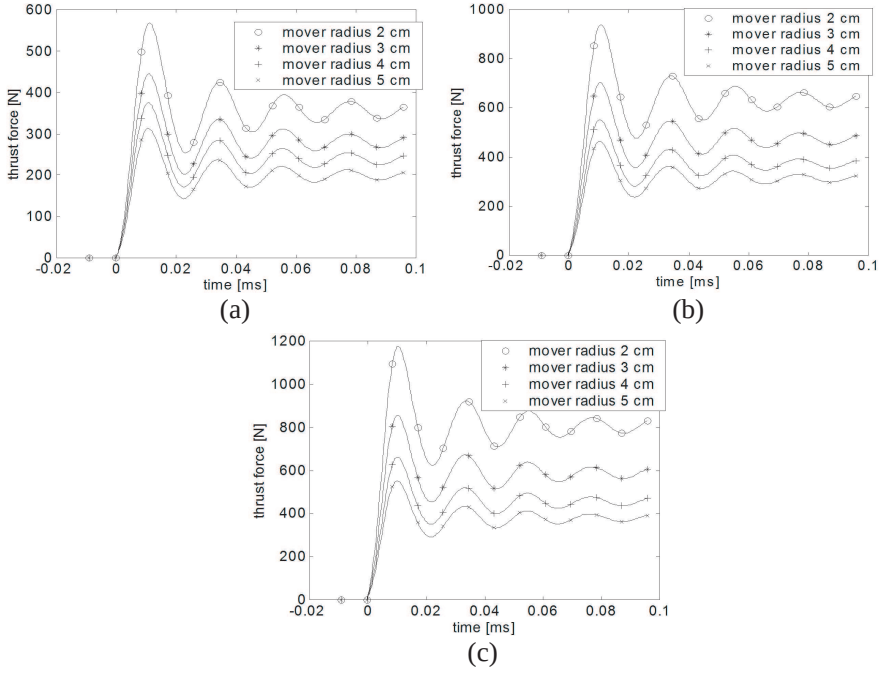

Figure 4. Transient waveforms of thrust force. (a) Teeth: 8 mm wide; slots: 5.5 mm long, 39.4 mm deep; (b) teeth: 6.8 mm wide; slots: 6.7 mm long, 29 mm deep; (c) teeth: 5.5 mm wide; slots: 8 mm long, 23.8 mm deep.

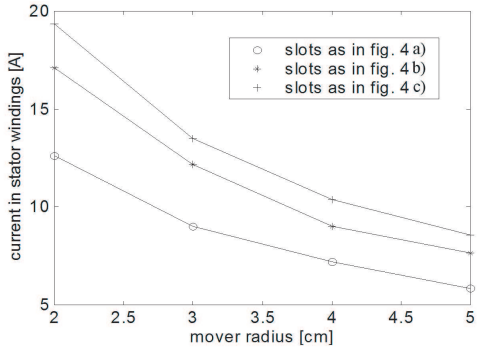

Figure 5. Currents in TLIM for different shapes of slots and mover radii.

approximation we can assume that the absorbed current is inversely proportional to the radius. The thrust force quadratically depends on the current and is approximately linear with respect to the surface of the conductive sheet on the mover. As a result the thrust is inversely proportional to the radius. This is true if saturation, that is likely to occur in motors with small radius, is not considered. Conversely, if we keep constant the maximum value of the flux density in the motor, the dependence of the thrust with the radius is approximately linear. This condition requires that the feeding voltage is approximately proportional to the radius.

3.2. Steady Response

These considerations are confirmed by the results reported in Fig. 5 which shows the absorbed currents in steady conditions corresponding to Figs. 4(a)–4(c).

Figure 5 shows that at given feeding voltage, motors with small radii absorb higher currents; so they are able to produce a given force with smaller voltage with respect to a motor with a greater radius. Thermal stresses may appear in small radii TLIMs; electric insulation are subject to stress in motor with large radii.

The dependence of the thrust force on the conductor thickness of the mover has also been investigated. Fig. 6(a) shows the thrust force for a TLIM characterized by teeth 6.8 mm long with slots 6.7 mm wide and 29 mm deep, the inner radius of the mover of 3.6 cm and iron thickness of 2 mm. The curves in the figure are obtained for different values of conductivity. Feeding voltage is 220 V at 50 Hz. Fig. 6(b) shows the currents absorbed by the motor corresponding to the same

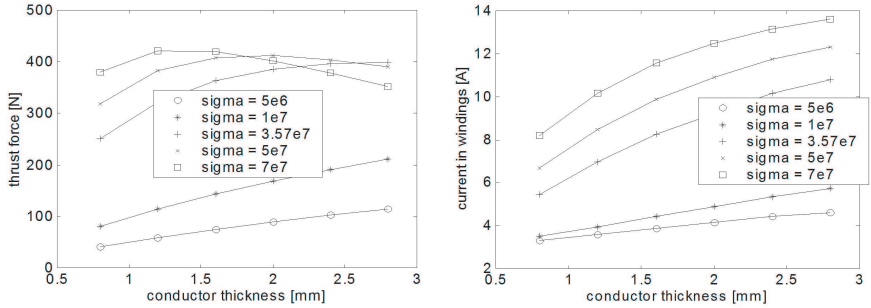

(a) (b)

Figure 6. Thrust force (a) and current in primary windings (b) for different values of the conductivity and thickness of the conductive part of the mover.

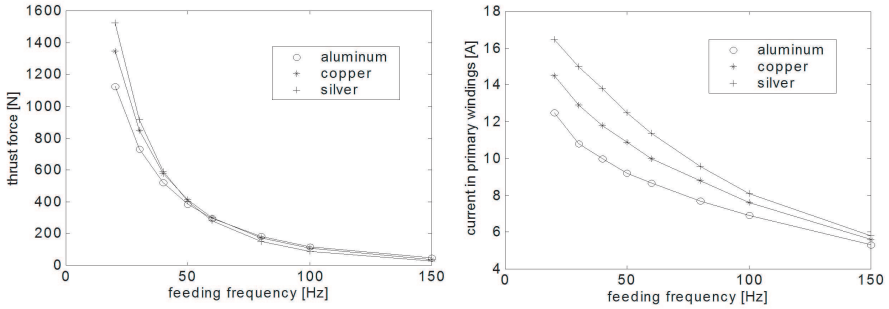

(a) (b)

Figure 7. Force on the mover (a) and current in the primary windings (b) for different materials.

operating condition as those of the previous figure. The curves in Fig. 6(a) that correspond to the three highest values of conductivity (aluminum, copper and silver) show the presence of maxima. The values of thickness of the conductive part of the mover and of the conductivity of the material corresponding to these maxima should be used in the design of the TLIM.

Figure 7(a) shows the thrust force as a function of the feeding frequency for a thickness of the conductive part of the mover of 2 mm and for three different materials (aluminum, copper and silver). Fig. 7(b) shows the currents in the primary windings under the same operating condition as Fig. 7(a). As expected the ratios $\left[\text{thrust force}/\text{current}^2\right]$ are curves with negative slope.

4. CONCLUSIONS

The Fourier transform has been applied in this paper to obtain the transient behavior of a TLIM at standstill taking into account the finite length of the stator windings. The main electromechanical quantities involved in this operating condition have been examined. The transient waveform of the thrust force on the mover reaches its maximum after few milliseconds; this makes attractive the use of TLIMs as fast actuators. In the related operating conditions is of great importance the promptness of the system at standstill while its behavior at steady state is less important. The analysis of the influence of the slots shape on the stator leakage inductance has highlighted the need for wide slots of limited depth. Further useful information for the design procedure have been obtained by varying the thickness and the conductivity of the conductive part of the mover and by varying the frequency of the feeding three phase voltage generator.

REFERENCES

1. De Groot, D. J. and C. J. Heuvelman, "Tubular linear induction motor for use as a servo actuator," *Proc. IEE*, Vol. 137, Part B, No. 4, 273–280, 1990.
2. Duncan, J., "Linear induction motor equivalent circuit model," *Proc. Inst. Elect. Eng.*, Vol. 130, Part B, No. 1, 5157, Jan. 1983.
3. Gieras, J. F., *Linear Induction Drives*, Clarendon, Oxford, UK, 1994.
4. Boldea, I. and S. A. Nasar, *Linear Motion Electromagnetic Systems*, Wiley, New York, 1985.
5. Nasar, S. A., et al., "Eddy-current losses in a tubular linear induction motor," *IEEE Trans. on Mag.*, Vol. 30, No. 4, 1437–1445, Jul. 1994.
6. Matyas, A. R., K. A. Biro, and D. Fodorean, "Multi-phase synchronous motor solution for steering applications," *Progress In Electromagnetics Research*, Vol. 131, 63–80, 2012.
7. Touati, S., R. Ibtiouen, O. Touhami, and A. Djerdir, "Experimental investigation and optimization of permanent magnet motor based on coupling boundary element method with permeances network," *Progress In Electromagnetics Research*, Vol. 111, 71–90, 2011.
8. Greig, J. and E. M. Freeman, "Travelling-wave problem in electrical machines," *Proc. IEE*, Vol. 114, No. 11, 1681–1683, Nov. 1967.

9. Tegopulos, J. A. and E. E. Kriezis, *Eddy Currents in Linear Conducting Media*, Elsevier, Amsterdam, 1985.
10. Barmada, S., A. Musolino, R. Rizzo, and A. Tellini, "Fields analysis in axysimmetric actuators," *IEEE Trans. on Mag.*, Vol. 36, No. 4, 1906–1909, Jul. 2000.
11. Barmada, S., A. Musolino, M. Raugi, and R. Rizzo, "Force and torque evaluation in hybrid FEM-MOM formulations," *IEEE Trans. on Mag.*, Vol. 37, No. 5, 3108–3111, Sep. 2001.
12. Musolino, A., "Finite-element method/method of moments formulation for the analysis of current distribution in rail launchers," *IEEE Trans. on Mag.*, Vol. 41, No. 1, 387–392, 2005.
13. Barmada, S., A. Musolino, M. Raugi, and R. Rizzo, "Analysis of the performance of a multi-stage pulsed linear induction launcher," *IEEE Trans. on Mag.*, Vol. 37, No. 1, 111–115, Jan. 2001.
14. Eastham, J. F., R. Akmese, D. Rodger, and R. J. Hill-Cottingham, "Prediction of thrust forces in tubular induction machines," *IEEE Trans. on Mag.*, Vol. 28, No. 2, 1375–1377, Mar. 1992.
15. EFFE, *User Manual*, Bathwick Electrical Design Ltd., UK, Sep. 2009.
16. Barmada S., A. Musolino, M. Raugi, and R. Rizzo, "Analysis of the performance of a combined coil-rail launcher," *IEEE Trans. on Mag.*, Vol. 39, No. 1, 103–107, 2003.
17. Lecointe, J.-P., B. Cassoret, and J.-F. Brudny, "Distinction of toothing and saturation effects on magnetic noise of induction motors," *Progress In Electromagnetics Research*, Vol. 112, 125–137, 2011.
18. Mahmoudi, A., N. A. Rahim, and W. P. Hew, "Axial-flux permanent-magnet motor design for electric vehicle direct drive using sizing equation and finite element analysis," *Progress In Electromagnetics Research*, Vol. 122, 467–496, 2012.
19. Jian, L., G. Xu, Y. Gong, J. Song, J. Liang, and M. Chang, "Electromagnetic design and analysis of a novel magnetic-gear-integrated wind power generator using time-stepping finite element method," *Progress In Electromagnetics Research*, Vol. 113, 351–367, 2011.
20. Musolino, A. and R. Rizzo, "Numerical analysis of brush commutation in helical coil electromagnetic launchers," *IET Science, Measurement and Technology*, Vol. 5, No. 4, 147–154, 2011.
21. Barmada, S., A. Musolino, M. Raugi, and R. Rizzo, "Numerical

simulation of a complete generator-rail launch system," *IEEE Trans. on Mag.*, Vol. 41, No. 1, 369–374, 2005.

22. Musolino, A., M. Raugi, and B. Tellini, "3-D field analysis in tubular induction launchers with armature transverse motion," *IEEE Trans. on Mag.*, Vol. 35, No. 1, 154–159, 1999.
23. Musolino, A. and R. Rizzo, "Numerical modeling of helical launchers," *IEEE Transactions on Plasma Science*, Vol. 39, 935–940, 2011.
24. Matrosov, V. M., A. Musolino, R. Rizzo, and M. Tucci, "A new passive maglev system based on eddy current stabilization," *IEEE Trans. on Mag.*, Vol. 45, No. 3, 984–987, 2009.
25. Musolino, A., R. Rizzo, E. Tripodi, and M. Toni, "Modelling of electromechanical devices by GPU accelerated integral formulation," *Int. J. of Num. Modelling: Electron. Networks, Devices and Fields*, Published online in Wiley Online Library (wileyonlinelibrary.com), 1–21, 2012, DOI:10.1002/jnm.1860.
26. Musolino, A., R. Rizzo, E. Tripodi, and M. Toni, "Acceleration of electromagnetic launchers modeling by using graphic processing unit," *IEEE 16th EML Symposium Conference Proceedings*, Beijing, May 15–19, 2012.
27. Barmada, S., A. Musolino, M. Raugi, R. Rizzo, and M. Tucci, "A wavelet based method for the analysis of impulsive noise due to switch commutations in power line communication (PLC) systems," *IEEE Trans. on Smart Grid*, Vol. 2, No. 1, 80–89, Mar. 2011.
28. Barmada, S., A. Musolino, R. Rizzo, and M. Tucci, "Multi-resolution based sensitivity analysis of complex non-linear circuits," *IET Circuits, Devices and Systems*, Vol. 6, No. 3, 176–186, 2012.
29. Di Puccio, F., "Permanent magnet bearing design: Optimising the magnetisation direction," *Int. Jour. Appl. Mech. and Eng.*, Vol. 9, No. 4, 655–674, 2004.
30. Kostenko, M. and L. Piotrovsky, *Electrical Machines*, MIR Publishers, Moscow, 1974.
31. Liwschitz, M., *Electrical Machinery*, D. Van Nostrand, New York, 1946.
32. Calixto, W. P., B. Alvarenga, A. P. Coimbra, A. J. Alves, L. M. Neto, M. Wu, W. G. da Silva, and E. Delbone, "Carters factor calculation using domain transformations and the finite element method," *Int J. Numer Model El.*, Vol. 25, No. 3, 236–247, Jun. 2012.

33. Yamamura, S., *Theory of Linear Induction Motors*, John Wiley & Sons, 1972.
34. Musolino, A., R. Rizzo, and E. Tripodi, "Analytical model of a travelling wave multipole field electromagnetic launcher," *IEEE 16th EML Symposium Conference Proceedings*, Beijing, May 15–19, 2012.
35. Musolino, A., R. Rizzo, and E. Tripodi, "Analysis and design criteria of a tubular linear induction motor for a possible use in the electro-magnetic aircraft launch system," *IEEE 16th EML Symposium Conference Proceedings*, Beijing, May 15–19, 2012.
36. Abramovitz, M. and I. A. Stegun, *Handbook of Mathematical Functions*, Dover, New York, 1972.